THE VESTAL CATACLYSM. B. A. Cohen, NASA Marshall Space Flight Center, Huntsville AL 35812 (Barbara.A.Cohen@nasa.gov).

Introduction: The currently operating Dawn mission shows asteroid 4 Vesta to be an extensively cratered body, with craters in a variety of morphologies and preservation states The crater size-frequency distribution for Vesta, modeled using the lunar chronology and scaled to impact frequencies modeled for Vesta, shows that both the north and south pole areas are ancient in age [1].

We have in our meteorite collection products from 4 Vesta in the form of the HED (howardite, eucrite, diogenite) meteorites. The HED parent body globally differentiated and fully crystallized by ~4.56 Ga; subsequently, the eucrites were brecciated and heated by large impacts into the parent body surface, reflected in their disturbance ages [2, 3].

Dawn images have also shown that Vesta is covered with a well-developed regolith that is spectrally similar to howardite meteorites [4, 5]. Howardites are polymict regolith breccias made up mostly of clasts of eucrites and diogenites, but which also contain clasts formed by impact into the regolith. Impact-melt clast ages from howardites extend our knowledge of the impact history of Vesta, expanding on eucrite disturbance ages and helping give absolute age context to the observed crater-counts on Vesta.

Howardite Impact-melt Clasts: We characterized texture, bulk composition, mineralogy, and ages of individual clasts within howardites EET 87513, QUE 94200, GRO 95574 and QUE 97001 in 100-µm thick, polished sections. Several clasts proved to be eucritic, but most were impact-melt clasts having a fine-grained, microporphyritic groundmass containing anhedral, relic mineral grains. The groundmass is usually too fine-grained to directly analyze the plagioclase or mafic portions. The relic clasts are dominated by plagioclase and pyroxene, with minor olivine, chromite, and other minerals. Pyroxene grains are typically homogeneous and unexsolved. Plagioclase has a wide range of compositions between typical eucrites and diogenites. Several clasts have symplectic textures with glassy areas. In these clasts, plagioclase can be significantly K-rich. The impact-melt clasts have bulk compositions ranging in between the eucrites and diogenites (Fig. 1), consistent with their interpretation as impact melt rocks made up of varying contributions of Vesta's two main lithologies.

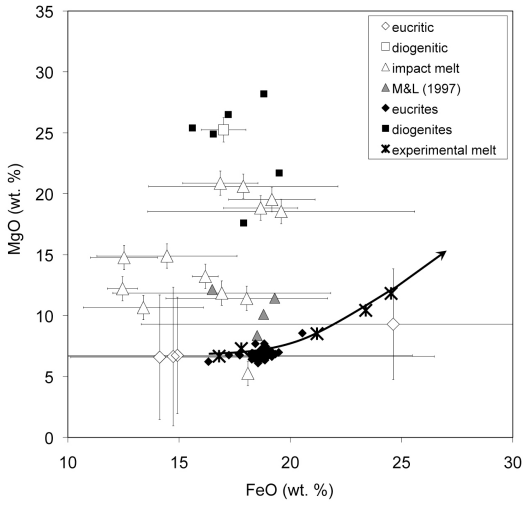

Fig. 1. The bulk composition of the impact-melt clasts is intermediate between eucrites and diogenites.

Samples were irradiated and step-heated using a CO_2 laser. Data were corrected for system blanks, decay time, and reactor-induced interferences. Resolution of cosmogenic and trapped argon components was attempted following [6, 7], but cosmogenic ^{36}Ar is not well-correlated with any specific component in these samples [3], so this correction was not pursued further. Most ages are reported from isochrons, which do not assume a trapped component; those with plateau ages assume a trapped contribution of zero and are therefore upper limits. Table 1 shows the new howardite ages, including the first impact-melt ages from HED meteorites. All of the new impact-melt ages fall between 4.0 and 3.5 Ga, and most are distinct from one another, meaning they sample different impact events on the surface of 4 Vesta.

Discussion: Our new impact-melt ages fall well within the age distribution of all HED impact-reset rocks, which features a short, intense spike at 4.48 Ga followed by a period of relative quiescence, then a ramping up of impact-reset ages between about 4.0 and

Table 1. Ages and types of samples in this study.

Sample	Type	Age (Ma)
A01	eucrite	3600 ± 300
A10	Impact melt	3330 ± 120
B5	eucrite	3200 ± 200
B11	breccia	3350 ± 60
B14	eucrite	2820 ± 190
B16	Impact melt	3560 ± 100
C14	eucrite	3540 ± 70
C15	Impact melt	3630 ± 130
C17	Impact melt	3960 ± 50
D01	Impact melt	3960 ± 30
D08	Impact melt	3720 ± 80
D11	Impact melt	3310 ± 130
D17	Impact melt	4000 ± 200
D19	Impact melt	3760 ± 150
D23	Impact melt	3600 ± 300

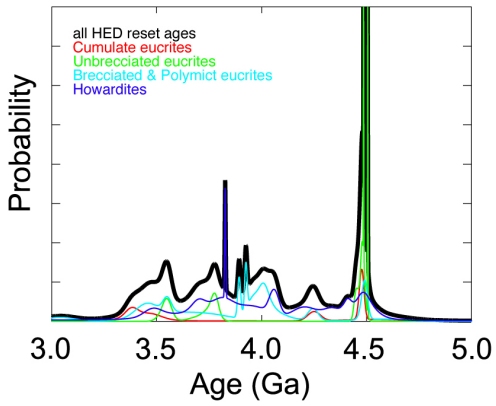

Fig. 2. Ideogram of Ar-Ar reset ages for HED meteorites, including 14 new ages.

3.5 Ga (Fig. 2). Bogard and Garrison [8] suggested that the early spike, largely contributed by unbrecciated eucrites, represents a single large impact into Vesta that caused widespread resetting and may have formed a secondary parent body, protecting the unbrecciated eucrites from further processing in the Vesta regolith.

Impact-reset ages in the HEDs are consistent with a quiescent period in the main belt, followed by increased activity in the period of the late heavy bombardment. However, this seems at odds with the observed crater distribution on Vesta, which shows a range of ages rather than a single resurfacing event. Rather, we suggest that the age distribution of HED meteorites only incompletely records the impact history of Vesta, because of the difficulty of resetting rock ages by collisions in the main belt.

Reset of argon-based ages is a diffusion-controlled process, where a combination of temperature and time is required to lose daughter Ar from the crystal lattice sites originally occupied by K cations. Eucrites (and howardites) contain K (and therefore Ar) primarily in pyroxene and plagioclase. Recent work on diffusion coefficients in these minerals [9, 10] permit a quick look at closure temperatures and diffusion rates in these minerals, which in turn constrains the conditions required to reset the age of these rocks.

Fig. 3 shows the time required to completely diffuse Ar (fully reset) through each mineral across different lengthscales. At elevated temperatures, plagioclase can diffuse Ar fairly rapidly, but pyroxene requires a very high temperature to fully reset, even on the single grain scale. At higher temperatures, complete melting occurs, which readily allows Ar diffusion and age reset. Temperatures in the range that enable significant diffusion over timescales of 1-100 years (fast cooling of a post-impact blanket) are relatively high, in the range of 1000°C.

Whether temperatures reach this high in the target rock is a strong function of the impact velocity. Typical impact velocities between objects in the main belt is about 5 km [11], which imparts far too little energy to raise the temperature of the target material above the closure temperature of typical eucrite minerals (300-400°C for plagioclase, 600-700°C for pyroxene). Of course, there is a velocity distribution, where some small fraction of impactors may achieve this high velocity, but these must be comparatively rare.

Our new impact-melt analyses deepen this story. In order to melt material on the surface of Vesta, an impact must have higher velocity still. The tail of the main belt velocity distribution doesn't stretch far enough to enable so much melt from so many different impact events spaced so closely in time. Therefore, we contend that these impact-melt clasts, and probably most of the impacts in this period, must be the result of highly velocitous impacts, possibly from an excited main belt (E-Belt) [12] or originating outside the main belt, as in the cometary flux of the Nice model [13]. Either way, howardite impact-melt clast ages record an unusual period of bombardment in the inner solar system beginning at around 4.0 Ga.

References: [1] Schenk, P.M., et al. (2011) *GSA Abstracts with Programs* **43**, 573. [2] Bogard, D.D. and D.H. Garrison (1993) *Meteoritics* **28**, 325-326. [3] Bogard, D.D. and D.H. Garrison (2003) *MAPS* **38**, 669-710. [4] Mittlefehldt, D.W., et al. (2011) *GSA Abstracts with Programs* **43**, 574. [5] McSween, H.Y., et al. (2011) *Geological Society of America Abstracts with Programs* **43**, 572. [6] Garrison, D., S. Hamlin, and D. Bogard (2000) *MAPS* **35**, 419-429. [7] Swindle, T.D., et al. (2009) *MAPS* **44**, 747-762. [8] Bogard, D.D. and D.H. Garrison (1999) *MAPS* **34**, 451-473. [9] Cassata, W.S., P.R. Renne, and D.L. Shuster (2009) *GCA* **73**, 6600–6612. [10] Cassata, W.S., P.R. Renne, and D.L. Shuster (2011) *EPSL* **304**, 407–416. [11] Farinella, P. and D.R. Davis (1992) *Icarus* **97**, 111-123. [12] Bottke, W.F., et al. (2010). *LPSC* **41**, 1533. [13] Gomes, R., et al. (2005) *Nature* **435**, 466-469.

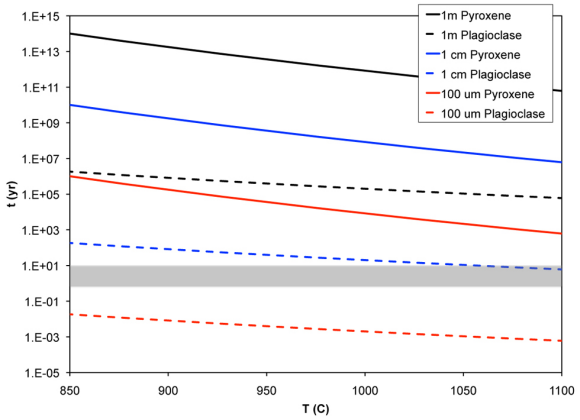

Fig. 3. Temperature-time curves for complete Ar diffusion over different length scales.